



PERFORMANCE COMPARISON OF FUZZY- PSO AND FUZZY-GA FOR DOUBLE-GIRDER CRANE CONTROL

B. M. Abba¹ and I. O. Essiet².

¹Department of Electrical Engineering Technology School of Technology, Kano State Polytechnic, Kano-Nigeria.

²Department of Computer Engineering, Bayero University, Kano- Nigeria.

*Corresponding author email: bashirmabba82@kanopoly.edu.ng

Received: 31-03-2026

Revised: 12-05-2026

Accepted: 16-05-2026

Published: 07-06-2026

Abstract: Double-girder overhead cranes are essential in industries for material handling, but their nonlinear dynamics, under actuation, and payload swing complicate control. This paper presents two Mamdani-type fuzzy logic controllers (FLC) using expert operator knowledge for trolley positioning and sway control. The crane's nonlinearity was modelled via Euler-Lagrange and simulated in MATLAB/Simulink. Particle swarm optimization (PSO-FLC) and genetic algorithm (GA-FLC) tuned the FLC membership functions to minimize a composite cost function based on integral of time-squared error (ITSE). Simulation results showed PSO-FLC outperforms standalone FLC and GA-FLC. For position control, PSO-FLC achieves fastest settling time (3.8 sec), lowest overshoot (0.039%), and smallest error metrics. ITSE and ISE are reduced by 70% compared to standalone FLC, and by 43% (ITSE) and 40% (ISE) compared to GA-FLC. For sway control, PSO-FLC delivers 3.3 sec settling time, minimal overshoot (0.0049%), and negligible undershoot. IAE is reduced by 36% versus GA-FLC and 40% versus standalone FLC. Larger improvements in ITAE (44% and 49%) compared to IAE (36% and 40%) are significant, as ITAE penalizes steady-state error more heavily over time, indicating superior long-term error reduction and faster settling. Overall, PSO-FLC demonstrates the most effective strategy with superior precision, faster stabilization, and improved sway suppression for double-girder crane systems.

Key words: Double-girder crane; position- sway; fuzzy logic controller; particle swarm optimization; genetic algorithm

1 Introduction

Industrial control systems are essential to many different entities such as; Manufacturing, transportation, construction, nuclear plant, mining, production etc. Due to the occupational safety regulations and weight of the products, it is frequently not feasible to move semi-processed or processed goods in manufacturing regions using labour. Specialized machine known as cranes are used to transfer related products by rotating, ascending and descending, or on flat axes, in order to lift them and shift them to another location (Doğan, 2023).

A crane is a specialized machine used in industries, shipyards, high building construction, and nuclear plants to move heavy loads and dangerous materials. It is outfitted with chains or cables and sheaves. In the industrial sector, a crane's primary function is to carry

a heavy item from one location to another in the least amount of time while swinging as little as possible. In order to complete this duty, a skilled operator must delay till the load blocks swinging and use his or her experience to quickly block the swing at the proper place. Inability to control the crane could also result in mishaps and injure people. The cargo that the crane is holding is unconstrained to swing in a pendulum-like pattern while operating. Unwanted swings are caused by the crane's nonlinear characteristics, particularly during ascending and reaching the target position (Harb & Alenany, 2025).

Additionally, based on their beam construction, cranes are either single-girder or double-girder. The diagram of the double-girder overhead crane is shown in Figure 2. The fundamental role of overhead traveling cranes is to guarantee precise and quick to move items to a certain position in the least amount of time without any residual oscillation. It consists of two parallel

girders, and it is powered by an electric motor, trolley travels along the girders and supported by payload. (Zhang, 2023).

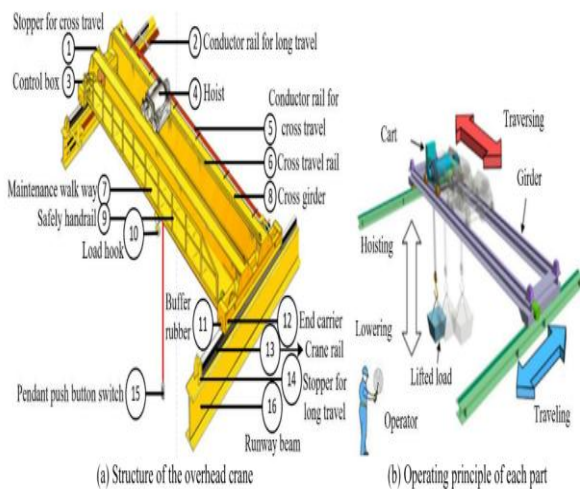


Figure 1: Structural diagram and mode of operation of the overhead crane (Automatisés *et al.*, 2024)

2 Background on crane control system

Many research have been conducted for overhead crane control system. Majority of cranes are manually operated. The overhead crane system's control has been the subject of numerous studies. Double girder bridge cranes are excellent for lifting very heavy loads, and in both indoor and outdoor operation, in a bridge or gantry setup, and are often applicable in industries such as mining, iron and steel production which are backbone of modern economies, rail yards, and shipping ports (Girder & Cranes, 2019).

A double-girder crane is type of overhead or bridge crane that supports a hoist and trolley by means of two parallel girders, or beams. The bridge is composed of two girder beams, each of which is supported by an end truck. The hoist and trolley typically operate on a horizontal bar that is mounted at top the bridge girders. Two types of double-girder cranes are: upper-level and lower-level running. The highest hook height and the biggest overhead space are provided by an upper-level running double-girder bridge crane. For a very heavy load applications where the crane must manage larger capacities and longer spans, double-girder cranes are advised.

Single girder crane is cheaper than the double girder cranes due to the more intricate design of the crane system's parts, such as trolley and host.



Figure 2: Double-girder crane system (Source:<https://krccranes.com/wpcontent/uploads/Aluminum-Plant-KRC-Double-Girder-Crane.jpg.webp>)

The dynamic equations of a crane are often time-varying, nonlinear differential equations (Alizada & Ozturk, 2023). These control systems' performance and stability demonstrate how crucial it is to choose the optimal approach and control scheme in line with the intended performance objective (Asad *et al.*, 2011).

(Mohamed *et al.*, 2022) established a control algorithm with the goal of accomplishing mass rate of production by moving the trolley accurately and by removing sway oscillations while taking safety precautions into account. The study produce non-linear mathematical model for a single-pendulum gantry crane with two stable control systems Proportional Integral Derivative (PID) and Proportional Derivative (PD) controllers, each of which has an inlet derivative filter. The simulated annealing algorithm (SAA) was used by (M. A. Mohammed *et al.*, 2021) to adjust the weighting matrices of the LQR in order to manage an overhead crane with respect to angle sway and position of the trolley. A Linear quadratic regulator (LQR) optimized by PSO was used to manage both swinging angle of a double pendulum crane system (Abdulhamid *et al.*, 2019). The main problem with building a LQR controller, according to the author, is that the Q and R parameters must be determined by the "rule of thumb" approach, which is quite time-consuming.

(Azmi *et al.*, 2019) presented the PID-PD based controllers for overhead cranes. The swinging of the load has created numerous challenges. when operating the overhead crane because of the pendulum-like settings. (Ahmad *et al.*, 2009) developed a dual control scheme for a gantry crane system to improve input

tracking and reduce payload swing. The system was modelled as nonlinear with uncertainties, using the Euler-Lagrange approach for dynamics. Two controllers were designed. A PD-based fuzzy logic controller (PD-FLC) to regulate the cart's position. A combined non-collocated PID and input shaper to control the swinging angle of the payload. The study evaluated the effectiveness of these controllers in managing crane movement and minimizing oscillations.

(Adeli, 2011) developed a hybrid controller that combines anti-swing control and position regulation. FLC and LQR were developed based on the Takagi-Sugeno fuzzy model of an overhead crane and the genetic algorithm. (Sun & Xie, 2020) designed a reinforcement learning-based backstepping control scheme (BSC) for the underactuated system for the crane system, controller's control gain is crucial since it affects how tracking errors converge. (Fu et al., 2023) employed a Stray lion swarm optimization algorithm (SLSO)-based fuzzy PID controller for overhead crane systems in order to enhance the fuzzy PID controller's performance.

(Shao et al., 2019) introduced a unique anti-swing and placement control approach for overhead cranes to address the nonlinear and unpredictable challenges of the dynamics model the approach used two types of T-S fuzzy models based on sector nonlinear theory. (A. Mohammed et al., 2023) developed an overhead crane system and optimized to find an ideal input function of the crane jib by genetic algorithm approach to tackle the problem of large swing angle a non-zero initial conditions. (Sharma, 2020) integrated and optimised FLC with the Enhanced Binary Bat Optimization algorithm (BBOA) to improve or modify the parameters of the fuzzy logic controller with the Priority Fitness Scheme (PFS) in gantry crane system.

Neural network was used by (Kozhubaev et al., 2023) in bridge crane operation for predicting the behaviour of the lifted load. (Esleman et al., 2021) developed a Bees algorithm method and genetic algorithm. The overhead crane's horizontal and swinging movements was managed using a fuzzy logic controller. A metaheuristic approach was used by (Cao et al., 2023) to optimize fuzzy logic controller with Proportional integral FLC-PI controllers to get the ideal and excellent performance of the control systems.

This research employs a fuzzy logic controller based on an optimization algorithm technique, in order to achieve high precision and stability of the double-girder crane system. The primary challenge in a double-girder overhead crane system is how to

precisely and swiftly position payloads while controlling the excessive load swing. This work has opted for fuzzy control due to some shortcomings in the conventional PID control method concerning nonlinearity and disturbance rejection. Particle swarm optimization tuned fuzzy logic controller (PSO-FLC) to minimize the objective function through the parameter tuning of the membership function, with a focus on attaining minimal rise time, settling time, and overshoot. Additionally, the performance metrics would be compared with the genetic algorithm tuned fuzzy logic controller (GA-FLC) technique. Hence, this paper chosen the PSO/GA algorithm to optimize the fuzzy logic controller for performance metrics.

3 Methodology

This paper has three methodical approaches:

- (a) System's general equation to regulate the trolley's horizontal movement, based on the principle that controlling trolley motion indirectly controls payload sway and was adopted from (Sharma, 2020).
- (b) Implementing a fuzzy logic controller (FLC) and optimizing using Particle swarm optimization tuned fuzzy logic controller (PSO-FLC) to minimize the cost function through the parameter tuning of the membership function, and comparing with the Genetic algorithm tuned fuzzy logic controller (GA-FLC) was used to minimize the cost function through the parameter turning of the membership function of the FLC for comparative analysis.
- (c) Evaluating and comparing the PSO-FLC controller with the GA- FLC based controller across key metrics: application, flexibility, safety and performance.

3.1 Mathematical model and free-body diagram of crane system

Free-body diagram of double-girder crane system is shown in Figure 3, where F or u represent the control force, $x(t)$ is the horizontal position of the trolley; M and m are the mass of the trolley and the payload, respectively; l is the length of the cable, $\theta(t)$ (or x_1) is the swing angle of the payload, $\dot{\theta}$ (or x_2) is the angular velocity of the payload, $\ddot{\theta}$ (or x_3) is the angular acceleration of the payload, \dot{x} (or x_4) is the velocity of the trolley, \ddot{x} acceleration of trolley and g denotes the gravitation acceleration.

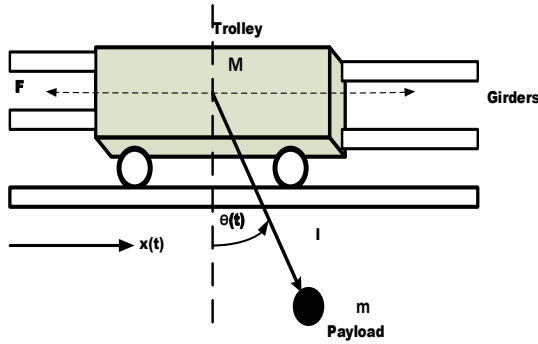


Figure 3: Double-girder crane system model designed in Microsoft Visio.

The Lagrange equation is given by the difference between the Kinetic energy T and potential energy V of the system.

$$L = T - V \tag{1}$$

Kinetic energy T;

$$T = \frac{1}{2} M \dot{x}^2 + \frac{1}{2} m (\dot{x}^2 + (l\dot{\theta})^2 + 2l\dot{x}\dot{\theta} \cos(\theta)) \tag{2}$$

Potential energy V;

$$V = mgl \cos(\theta) \tag{3}$$

Simplifying the kinetic energy

$$T = \frac{1}{2} (M + m) \dot{x}^2 + \frac{1}{2} ml^2 \dot{\theta}^2 + ml\dot{x}\dot{\theta} \cos(\theta) \tag{4}$$

Using the Euler- Lagrange equation for x and θ

$$\frac{d}{dt} \left(\frac{\partial L}{\partial \dot{x}} \right) - \frac{\partial L}{\partial x} = F \tag{5}$$

$$\frac{d}{dt} \left(\frac{\partial L}{\partial \dot{\theta}} \right) - \frac{\partial L}{\partial \theta} \tag{6}$$

For x

$$(M + m)\ddot{x} + ml\ddot{\theta} \cos(\theta) - ml\dot{\theta}^2 \sin(\theta) = F \tag{7}$$

For θ

$$ml\ddot{x} \cos(\theta) + ml^2\ddot{\theta} - mgl \sin(\theta) = 0 \tag{8}$$

Equation (8) become;

$$\ddot{\theta} = \frac{g \sin(\theta) - \dot{x} \cos(\theta)}{l} \tag{9}$$

Substitute $\ddot{\theta}$ into equation (7)

$$(M + m)\ddot{x} + ml \left(\frac{g \sin(\theta) - \dot{x} \cos(\theta)}{l} \right) \cos(\theta) - ml\dot{\theta}^2 \sin(\theta) = F \tag{10}$$

$$\ddot{x} = \frac{F + ml\dot{\theta}^2 \sin(\theta) - mgsin(\theta)\cos(\theta)}{M + m - m\cos^2(\theta)} \tag{11}$$

Solving $\ddot{\theta}$, and from equation (9), substitute the expression for \ddot{x} ;

$$\ddot{\theta} = \frac{g \sin(\theta)}{\cos(\theta)} - \frac{\dot{x}}{l \cos(\theta)} \tag{12}$$

3.2 State-space representation

The state vector x and input u are;

$$X = \begin{bmatrix} x_1 \\ x_2 \\ x_3 \\ x_4 \end{bmatrix}, \quad F \text{ or } u = \text{control force}$$

The derivatives of the state variables are;

$$\dot{X} = \begin{bmatrix} \dot{x}_1 \\ \dot{x}_2 \\ \dot{x}_3 \\ \dot{x}_4 \end{bmatrix} = \begin{bmatrix} x_2 \\ aux_{01} \\ x_4 \\ aux_{02} \end{bmatrix} \tag{13}$$

Substituting the linearized forms of aux_{01} and aux_{02}

$$\dot{x}_2 = x_2 \tag{14}$$

$$\dot{x}_3 = \frac{-u + (M+m)gx_1}{Ml} \tag{15}$$

$$\dot{x}_4 = x_4 \tag{16}$$

$$\dot{x}_4 = \frac{u}{Ml} - \frac{mgx_1}{Ml} \tag{17}$$

3.3 State-space Equations

Transforming the above equations into the matrix form;

$$\dot{X} = Ax + Bu \tag{18}$$

where,

$$A = \begin{bmatrix} 0 & 1 & 0 & 0 \\ [(M + m)g]/Ml & 0 & 0 & 0 \\ 0 & 0 & 0 & 1 \\ -mg/Ml & 0 & 0 & 0 \end{bmatrix},$$

$$B = \begin{bmatrix} 0 \\ -1/(Ml) \\ 0 \\ 1/(Ml) \end{bmatrix} \text{ and } x = \begin{bmatrix} x_1 \\ x_2 \\ x_3 \\ x_4 \end{bmatrix}$$

$$\dot{X} = \begin{bmatrix} 0 & 1 & 0 & 0 \\ [(M+m)g]/Ml & 0 & 0 & 0 \\ 0 & 0 & 0 & 1 \\ -mg/Ml & 0 & 0 & 0 \end{bmatrix} \begin{bmatrix} x_1 \\ x_2 \\ x_3 \\ x_4 \end{bmatrix} + \begin{bmatrix} 0 \\ -1/(Ml) \\ 0 \\ 1/(Ml) \end{bmatrix} * u \quad (19)$$

The system is linearized around an equilibrium position, it was unstable equilibrium position where all state variables are zero, insignificant deviations from this point, nonlinear terms become negligible, small angle approximation eliminates nonlinearities, making the model linear in the state variables, higher orders terms such as $\dot{\theta}^2 \sin(\theta)$ (centrifugal force) and other products of state variables are dropped because they are of second order, the linear model enable the use of linear design methods for stabilization and performance tuning. The linearized equation conforms to the standard linear time-invariant (LTI) form, which is required for many analyses and design techniques.

3.4 System design and implementation

Double-girder crane linearized state-space representation of the system was simulated in MATLAB/Simulink. Based on the state-space in equation (19), it has four states as follows;

$$\begin{bmatrix} x_1 \\ x_2 \\ x_3 \\ x_4 \end{bmatrix} = \begin{bmatrix} \theta(\text{Payload swing angle}) \\ \dot{\theta}(\text{Angular velocity of the payload}) \\ x(\text{Trolley position}) \\ \dot{x}(\text{Trolley velocity}) \end{bmatrix}$$

Force applied to the trolley is the control input u . A common and effective strategy is to use two separate fuzzy logic controllers.

Table I: System model parameters involved in the simulation (Sharma, 2020)

| Parameters | Values |
|---------------------------------|----------------------|
| Mass Trolley (M) | 5kg |
| Payload mass (m) | 1kg |
| Length of the payload cable (l) | 0.75m |
| Gravitational (g) | 9.81m/s ² |
| Damping coefficient (b) | 12.32 Ns/m |

3.5 System modelling and Simulation

The simulation was conducted in MATLAB/Simulink 2021a and followed a five-step process:

- (i) System Modelling: A state-space model was simulated using MATLAB’s built-in functions and a custom Euler integration method.
- (ii) Controller design: A Mamdani-type fuzzy logic controller (FLC) with triangular membership functions was implemented.
- (iii) PSO optimization: Particle swarm optimization (PSO) was applied to tune the FLC’s membership function parameters, aiming to minimize a defined cost function.
- (iv) Comparative analysis: A Genetic algorithm (GA-FLC) was implemented to provide a performance comparison with the PSO tuned controller (PSO-FLC)
- (v) Performance evaluation: The controllers were assessed using four standard error-based metrics Integral of time absolute error (ITAE), Integral absolute error (IAE), Integral squared error (ISE), and Integral time squared (ITSE) which integrate system error over time. The optimization goal was to minimize these values, thereby refining the system's response characteristics.

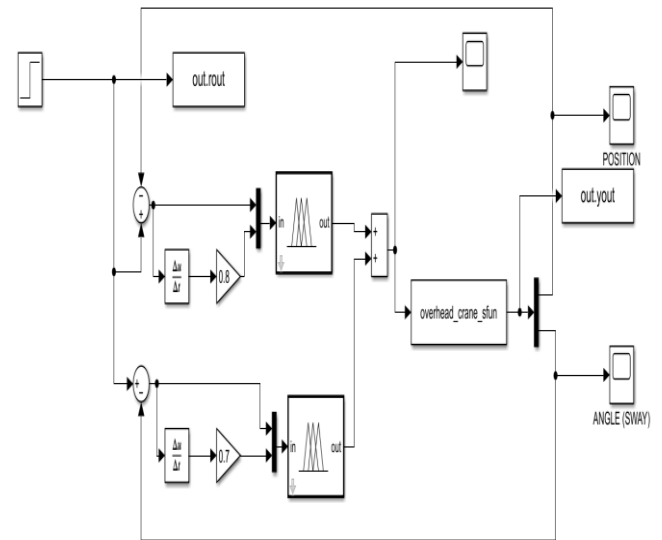


Figure 4: Proposed block diagram of Double-girder crane system designed in MATLAB/Simulink.

3.6 Design of Mamdani fuzzy logic controllers

MATLAB/Simulink was employed to design the FLC by using fuzzy logic toolbox. A common and effective strategy is to use two separate fuzzy logic controllers, the following procedures were conducted for the design of the controllers;

Step one: Problem definition and controller structure

Sway angle controller (FLC θ), Primarily responsible for damping the payload sway. Its inputs are the swing angle θ (x_1) and swing rate $\dot{\theta}$ (x_2). Its output is a control force F_θ . Fuzzy logic controller for position controller was used to move the trolley to the target position. Its inputs are the position error e_x (x_3) and the trolley velocity e_{dx} (x_4). Its output is the primary force F_x . The total control force u is the sum of these two forces, $u = F_\theta + F_x$. This structure allows the sway controller to actively dampen oscillations while the position controller does its job.

Step two: Fuzzification (Defining fuzzy sets)

This is defined as the linguistic variables with their membership functions for all inputs and outputs, triangular membership functions were selected for simplicity.

Step three: Rule Base (The ‘Brain’ of the FLC):

The rule base is a set of IF-THEN rules that capture the expert knowledge of how to control the crane. Rule base for sway controller (FLC θ) and rule base Position controller (FLC x) is shown in table II and table III.

Table II: Fuzzy rules table for the sway angle controller (FLC θ)

| | | | | | |
|----------------|----|----|----|----|----|
| $e\theta$ | NL | NS | Z | PS | PL |
| $\dot{\theta}$ | | | | | |
| NL | NL | NL | NL | NS | Z |
| NS | NL | NL | NS | Z | PS |
| Z | NL | NS | Z | PS | PL |
| PS | NS | Z | PS | PL | PL |
| PL | Z | PS | PL | PL | PL |

Twenty-five $5 \times 5 = 25$ rules could be generated from table II fuzzy rules for the sway angle controller and the following examples are stated as follows;

Rule 1: IF $e\theta$ is NL AND $\dot{\theta}$ is NL, THEN u or F_θ is NL. (If the payload is far to the left and accelerates to the left, pull the trolley left hard).

Rule 14: IF $e\theta$ is Z AND $\dot{\theta}$ is PS, THEN u or F_θ is PS. (If the payload is centred but moving right, apply a small force right to stop its motion).

Table III: Fuzzy rules table for the Position controller (FLC x)

| | | | | | |
|-----------|----|----|----|----|----|
| e_x | NL | NS | Z | PS | PL |
| \dot{x} | | | | | |
| NL | NL | NL | NL | NS | Z |
| NS | NL | NL | NS | Z | PS |
| Z | NL | NS | Z | PS | PL |
| PS | NS | Z | PS | PL | PL |
| PL | Z | PS | PL | PL | PL |

Twenty-five $5 \times 5 = 25$ rules could be generated from table III fuzzy rules for the position controller and the following examples are stated as follows;

Rule 6: IF e_x is NS AND \dot{x} is NL THEN output u or F_θ is NL. The position error is slightly negative (NS), but the velocity is negative large (NL), meaning the trolley is moving rapidly away from the target, even though it is currently near it. The controller must therefore apply a strong negative force (NL) to quickly arrest this motion and push the system back toward the target position.

Rule 13: IF e_x is Z AND \dot{x} is Z THEN output u or F_θ is Z (This is the target state. The position is exactly where it should be, and the system is stationary. Therefore, no control effort is needed (Zero output)).

3.7 Optimization using Particle Swarm Optimization (PSO)

The population "agents in the search domain" are randomly initialized at the beginning of PSO. The algorithm's success relies on the social behaviour of the particles in the swarm is the basis for how the PSO algorithm operates. In particle swarm optimization, a particle's velocity and therefore its position is updated by combining cognitive (personal best) and social (global best) components, guiding its movement through the search domain.

3.8 Optimization using Genetic algorithm (GA)

GA's primary goal is to replicate *natural selection* is the driving mechanism that results in the *survival of the fittest*. The solutions in GA are shown as chromosomes. The chromosomes are ordered from best to worst according on their fitness values

Table IV: Initial parameters setting of Particle swarm optimization PSO (Solihin et al., 2019)

| Parameters of PSO | Values |
|--------------------------------------|--|
| Inertia weight factor, ω | 0.7 |
| Cognitive constant, c_1 | 1.5 |
| Social constant c_2 | 1.5 |
| Swarm size or population size nPop | 50 |
| Maximum number of iterations (MaxIt) | 100 |
| Lower and upper boundaries | lb = [0.1, 0, 0.1, 0]; ub = [1, 0.7, 1, 0.9]; |
| Number of decision variables nVar | $k_1 k_2 k_3 k_4$ |

Table V: Initial parameters setting of Genetic algorithm (GA) (Solihin et al., 2019)

| Parameters of GA | Values |
|--------------------------------------|--|
| Maximum number of iterations (MaxIt) | 100 |
| Population size nPop | 50 |
| Crossover probability pc | 0.8 |
| Number of offspring (must be even) | $nc = 2 * \text{round}(pc * \frac{nPop}{2})$ |
| Mutation probability mp | 0.2 |
| Number of mutants | $nm = \text{round}(pm * nPop)$ $\gamma = 0.4$ |
| Crossover blend parameter | |
| Mutation rate mu | 0.1 |

4 RESULTS AND DISCUSSION

4.1 System model validation

The model validation includes state space simulation of the system model, fuzzy logic controller design using Mamdani-type fuzzy inference system (FIS) with triangular membership functions for simplicity, and optimization of the cost function using particle swarm optimization tuned fuzzy logic controller (PSO-FLC) by comparing its performance metrics

with genetic algorithm tuned fuzzy logic controller (GA-FLC).

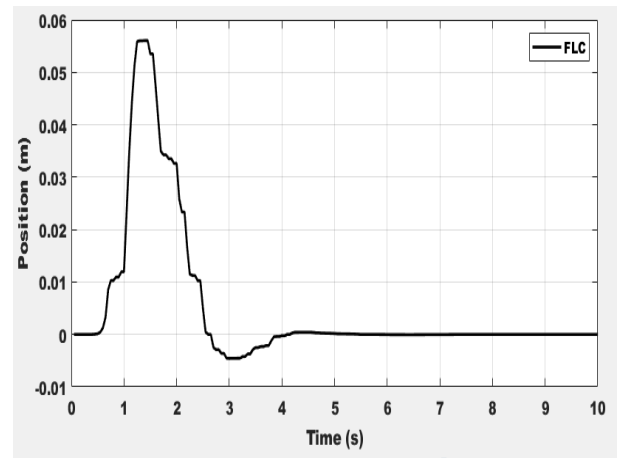


Figure 5: Position with fuzzy logic controller only without optimization.

Figure 5 shows a position with fuzzy logic controller only without optimization, it showed a fast, smooth, and accurate positioning with an overshoot of 0.056m, approximately 4.5 seconds settling time, undershoot of approximate -0.0057m and negligible steady-state error ideal characteristics for precise crane control where both trolley positioning and load angle suppression are critical.

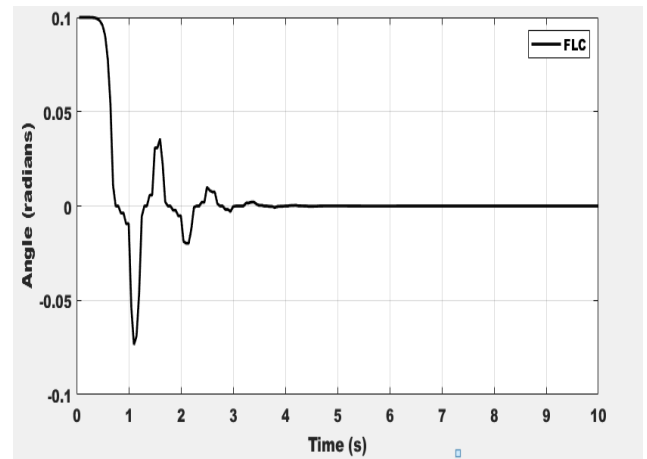


Figure 6: Angle (sway) with fuzzy logic controller only without optimization

Figure 6 shows FLC achieves an excellent anti-sway performance, by damping the load angle from 0.10 rad (5.7°) to zero within short period of time, and settling time of about 4 seconds with an overshoot of about 0.0048 radians and undershoot of approximate -0.078 radians. This demonstrates an effective fuzzy logic control design for the double-girder crane system guaranteeing safe and precise load positioning.

4.2 Result of the convergence analysis

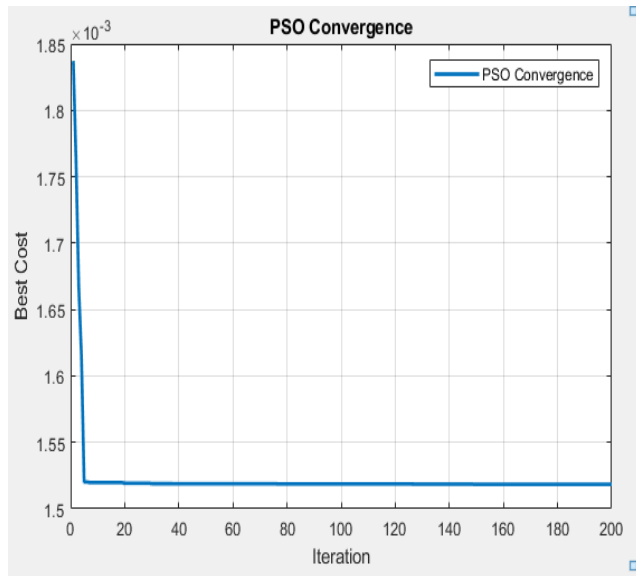


Figure 7: PSO-FLC convergence curve

Figure 7 shows the PSO-FLC convergence curve. The best cost (the objective function value) is shown on the vertical (y) axis, and the iteration number 200 is on the horizontal (x) axis. It indicates an effective convergence, reducing best cost by approximately 17% over 200 iterations. The smooth, monotonic (no oscillation or spikes) descent indicates stable optimization with no premature convergence or instability.

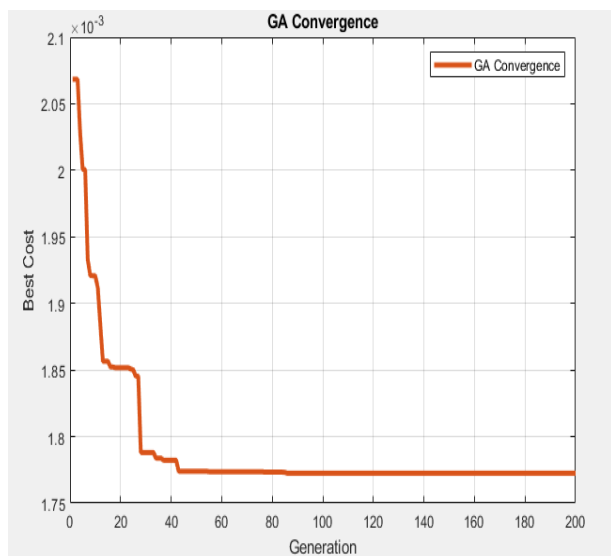


Figure 8: GA-FLC convergence curve

Figure 8 illustrates the convergence curve behaviour of a genetic algorithm over 200 generation, which is typically noisier and slower than PSO, reflecting its explorative nature through genetic operators. Even though GA start with a better initial solution, it often

fails to refine as precisely as PSO, resulting in a higher final best cost and less stable convergence, making PSO generally more suitable for fine-tuning FLC parameters in crane control application.

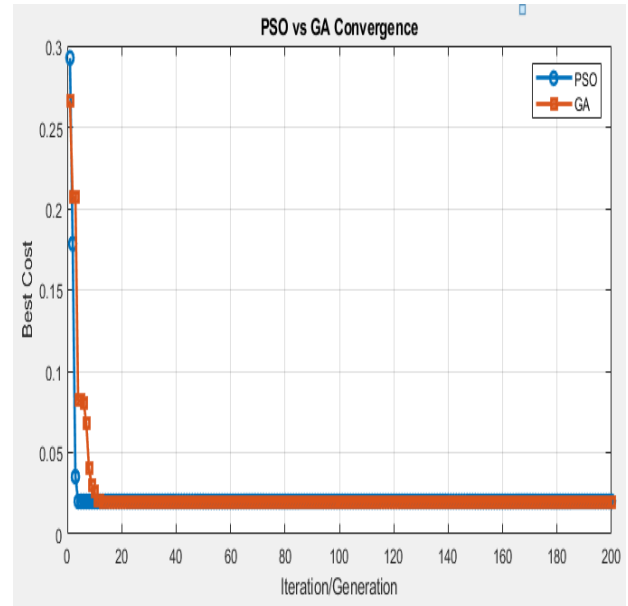


Figure 9: Comparison analysis between PSO-FLC and GA – FLC.

Figure 9 shows PSO significantly outperforms GA in terms of final solution quality (60-70% lower best cost), convergence speed (3 times faster), and stability of improvement. In PSO-FLC between 5 to 200 iterations the best cost started approximately high around 0.25 to 0.30 and later dropped quickly within the approximate 20 iterations, between iteration 5 and almost 40 to 60, PSO made of its improvement, reaching a best cost of roughly 0.1 or less. From 60 to 200 iterations, PSO plateaued that is very little to no further improvement, the curve flattened out, showing premature convergence and reaching a local minimum.

For GA-FLC between 10 to 200 iterations, it showed that GA started with a worse initial best cost than PSO roughly in 0.28 to 0.3 and converged more slowly, between 10 to 100 iterations, GA’s best cost decreased steadily but more gradually than PSO. After about 100 to 120 iterations, GA continued improving slightly beyond PSO’s plateau.

The PSO tuned FLC provided superior anti- sway control and precise positioning compared to the GA-tuned counterpart. PSO is the clear choice for achieving optimal crane controller parameters.

Table VI: Convergence analysis – Iteration versus Best cost (fuzzy logic controller tuning)

| Iteration | PSO Best Cost | GA Best Cost | Performance Gap (GA - PSO) |
|-----------|--------------------|--------------------|------------------------------------|
| 0 | 0.28 – 0.30 | 0.20 – 0.22 | GA better by ~0.08 |
| 20 | 0.10 – 0.12 | 0.15 – 0.17 | PSO better by ~0.05 |
| 40 | 0.03 – 0.05 | 0.12 – 0.14 | PSO achieves 60% lower cost |
| 60 | 0.02 – 0.03 | 0.10 – 0.12 | PSO significantly better |
| 100 | 0.01 – 0.02 | 0.07 – 0.09 | PSO maintains advantage |
| 150 | 0.00 – 0.01 | 0.06 – 0.08 | PSO approaches optimal |
| 200 | 0.00 – 0.02 | 0.05 – 0.07 | PSO final cost ~70% lower |

Table VI illustrated a convergence analysis – Iteration versus Best cost (fuzzy logic controller tuning), initially at iteration 0, GA begins with a lower best cost (0.20 to 0.22) than PSO with (0.28 to 0.30), so GA is better at the beginning of the iteration. Then from iteration 20 onward PSO overtakes GA, achieving favourably cost, while GA’s improvements are lower. By 200 iteration PSO’s best cost approached zero (0.00 to 0.02), whereas GA remains at 0.05 to 0.07, making PSO’s final cost approximately 70% lower than GA’s. Therefore, PSO converges faster and to a much better optimally than GA in tuning FLC.

4.3 Performance of the optimized fuzzy logic controller using Particle swarm optimization (PSO)

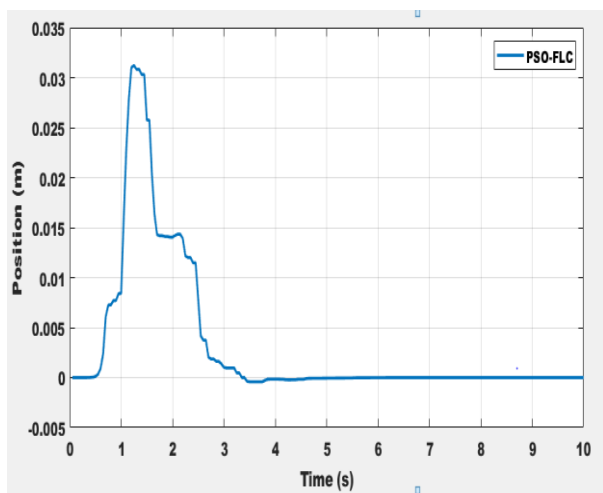


Figure 10: Position response with PSO-FLC optimized control

A fuzzy logic controller was optimized or fine-tune by using particle swarm optimization to achieve the optimal system performance under control.

Figure 10 compares the position plot response of the optimized FLC by PSO. The optimized controller achieves noticeable improved performance, where by the overshoot reduced from 0.056m to 0.032m, settling improves from 4.3 sec. to 3.8sec. and with very negligible undershoot. Also, oscillation was dampened rapidly following a smoother more stable behaviour with faster target positioning.

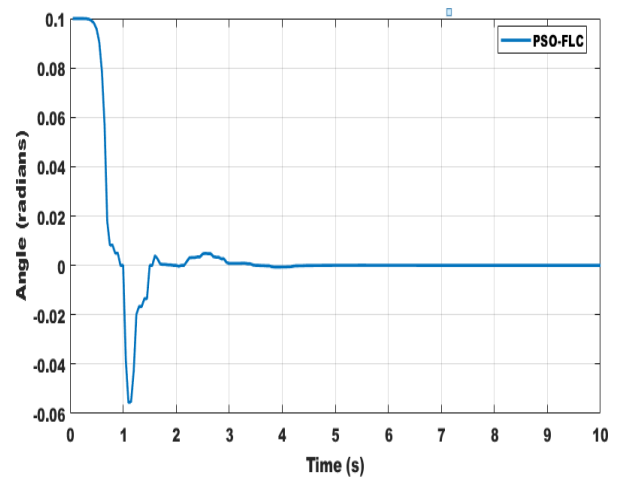


Figure 11: Angle response with PSO- FLC optimized control.

Figure 11 above shows the angular displacement response of the optimised controller PSO-FLC in radians. A significant amount of undershoot was observe with a value of -0.058 radians and an overshoot of 0.0049 radians. The time it takes for the oscillations to settle within a small percentage of the final value which is about 3.3sec. The response starts at a non-zero value of approximately 0.1 radians at $t = 0$ sec. This illustrates that the system had injected by disturbance (signal builder) before the step input was applied. The system's angle oscillates around its final steady-state value. This oscillatory behaviour, which decays over time, is a defining characteristic of an underdamped system. The system first drops below the steady-state value, with a significant undershoot of about -0.058 radians at approximately $t = 1.4$ sec. It then oscillates, with negligible overshoots and smaller undershoots, until it settles.

4.4 Performance of the optimized fuzzy logic controller using Genetic algorithm (GA)

Genetic algorithm (GA) was applied to optimize the fuzzy logic controller, for comparison with PSO.

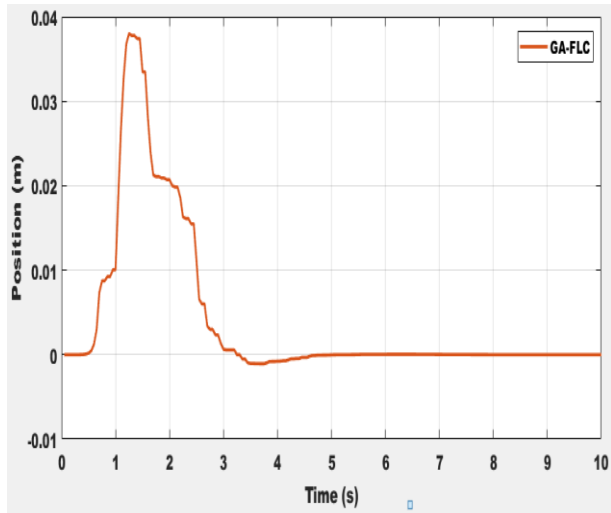


Figure 12: Position control response with GA-FLC

Figure 12 shown above is the response of the system's position using the GA-tuned controller. The transient response is the system's initial behaviour before it settles. The response rises very quickly, reaching a peak of approximately 0.039m at 0.0282sec. There is an overshoot, where the position exceeds the final desired value of 0m, with the overshoot of 0.039m. The system shows a complex settling behaviour. After the initial large oscillation, there's a smaller oscillation between $t = 1.5\text{sec.}$ and $t = 2.5\text{sec.}$ before it finally settles at the desired position. The system appears to settle at approximately 4.3 sec.

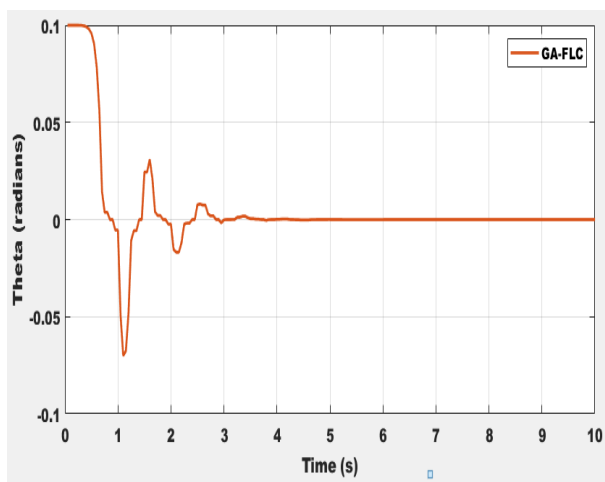


Figure 13: Angle control response GA-FLC

Figure 13 provide a graph of optimized controller using GA-FLC. The system has an overshoot of approximately 0.038 radians and takes roughly 3.8 sec. settling time. The system starts at an initial angle of 0.1 radians and has a large undershoot of about -0.075 radians. The oscillations are damped much more quickly. The system reaches its steady-state value with fewer oscillations and a faster decay. The system settles significantly faster, with the oscillations effectively dying out by 2-3 sec. which is a substantial improvement over the 4 sec. of the FLC without optimization.

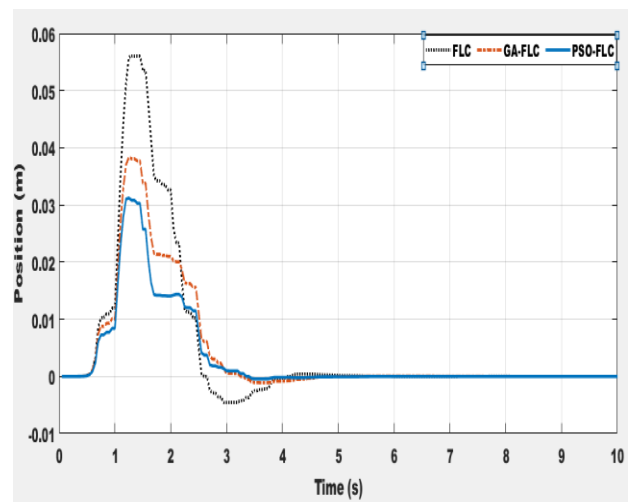


Figure 14: Position control response with standalone FLC, GA-FLC and PSO-FLC

The plots in figure 14 show the position response of a double-girder overhead crane system under three different control conditions. The system is inherently unstable, and fuzzy logic was used to stabilize it. The responses are; fuzzy logic controller without optimization (standalone) FLC, Genetic algorithm tuned fuzzy logic controller (GA-FLC) and Particle swarm optimization tuned fuzzy logic controller (PSO-GA)

The PSO optimized controller is the most effective, delivering the best performance with the lowest overshoot and the fastest settling time.

Table VII: Performance metrics for Position

| | Performance metrics for Position | | |
|-------------------|----------------------------------|---------------|----------------|
| | Fuzzy | Fuzzy with GA | Fuzzy with PSO |
| Settling time (s) | 4.5 | 4.3 | 3.8 |
| Rise time (s) | 0.0257 | 0.0282 | 0.0039 |
| overshoot (%) | 0.056 | 0.039 | 0.039 |
| Undershoot (%) | -0.0057 | -0.0010 | 0 |

Table VII details the transient response characteristics of three different control system designs; fuzzy logic controller (FLC without optimization), GA-FLC (Genetic algorithm optimized), and with PSO-FLC (Particle swarm optimization optimized) for position control a double-girder crane system.

Table VIII: Performance error metrics for Position

| Performance error metrics for Position | | | |
|--|----------|---------------|----------------|
| | Fuzzy | Fuzzy with GA | Fuzzy with PSO |
| IAE | 0.05567 | 0.04165 | 0.03126 |
| ITAE | 0.05702 | 0.04384 | 0.0309 |
| ITSE | 0.001687 | 0.0008811 | 0.0004993 |
| ISE | 0.002046 | 0.001022 | 0.000614 |

From table VIII above, fuzzy with PSO consistently achieves the lowest error values, indicating the most accurate and responsive control performance, outperforms fuzzy logic controller without optimization and is also more effective than GA in tuning the fuzzy controller's parameters for the positional control of the double-girder crane system. The reduction in integral-based errors particularly integral time squared-error ITSE and integral square error ISE, which penalize larger and sustained errors, implies that PSO yields a smoother and more precise positioning response with less overshoot and faster settling time.

Percentage improvement was evaluated as in (Aner et al., 2024) to reduce the system's error performance and to demonstrate the most effective strategy with superior precision and faster stabilization of the three different control conditions.

$$\begin{aligned}
 & \% \text{ Improvement in ITSE} \\
 &= \frac{(FLC \text{ standalone}) - (PSO - FLC)}{(FLC \text{ standalone})} \times 100\% \\
 &= \frac{0.001687 - 0.0004993}{0.001687} \times 100\% = 70\%
 \end{aligned}$$

$$\begin{aligned}
 & \% \text{ Improvement in ISE} \\
 &= \frac{(GA - FLC) - (PSO - FLC)}{(GA - FLC)} \times 100\% \\
 &= \frac{0.0008811 - 0.0004993}{0.0008811} \times 100\% = 43\%
 \end{aligned}$$

ITSE penalises large errors because of the squaring operation $e^2(t)$ and also places a greater weight on errors that last for long time due to time multiplication (t).

It is a very effective performance index for achieving a fast and stable response with long-term error. The satisfactory performance of optimized FLC is the one with the lower objective function value. (Solihin et al., 2019)

$$\begin{aligned}
 & \% \text{ Improvement in ISE} \\
 &= \frac{(FLC \text{ standalone}) - (PSO - FLC)}{(FLC \text{ standalone})} \times 100\% \\
 &= \frac{0.002046 - 0.000614}{0.002046} \times 100\% = 70\%
 \end{aligned}$$

$$\begin{aligned}
 & \% \text{ Improvement in ISE} \\
 &= \frac{(GA - FLC) - (PSO - FLC)}{(GA - FLC)} \times 100\% \\
 &= \frac{0.001022 - 0.000614}{0.001022} \times 100\% = 40\%
 \end{aligned}$$

The ISE criterion integrates the squared the error over time. By squaring the error, it places a much higher penalty on the large errors than on small ones (Solihin et al., 2019). This makes it good choice for applications where large deviations from the setpoints are unacceptable, such as double-girder crane system that requires minimal overshoot.

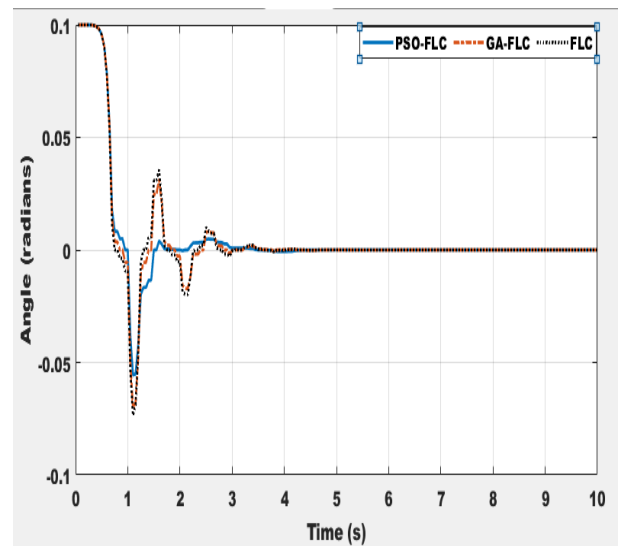


Figure 15: Sway angle (Theta) control with standalone fuzzy logic controller, GA-FLC and PSO-FLC

Figure 15 shows the response of the system, under different control conditions. The plots compare the

system response with fuzzy logic controller (standalone), Genetic algorithm (GA)tuned FLC and Particle swarm optimization (PSO) tuned FLC.

Table VII: Performance metrics for angle

| Performance metrics for Angle | | | |
|-------------------------------|---------|---------------|----------------|
| | Fuzzy | Fuzzy with GA | Fuzzy with PSO |
| Settling time (s) | 3.8 | 3.6 | 3.3 |
| Rise time (s) | 0.1538 | 0.02823 | 0.1521 |
| overshoot (%) | 0.0480 | 0.038 | 0.0049 |
| Undershoot (%) | -0.0780 | -0.075 | -0.058 |

From table VII. FLC (without optimization) has the longest settling time and highest overshoot of about 0.0480% indicating relatively a slower stabilization and large oscillation. GA-FLC demonstrates an improvement over FLC (without optimization) settling time, even though the rise time is faster than two strategies, and the overshoot of 0.038 % which also higher than the PSO-FLC. PSO-FLC shows an excellent performance among the three control strategies. It demonstrates shortest settling time of 2.9seconds lower than fuzzy (without optimization) with about 4 seconds and GA-FLC with 3.8 seconds which indicates faster stabilization, overshoot is also minimal at 0.0049% this indicates excellent damping and oscillation reduction.

Table VIII: Performance error metrics for Angle (sway)

| Performance error metrics for Angle | | | |
|-------------------------------------|---------|---------------|----------------|
| | Fuzzy | Fuzzy with GA | Fuzzy with PSO |
| IAE | 0.05697 | 0.05371 | 0.03410 |
| ITAE | 0.03881 | 0.03471 | 0.0196 |
| ITSE | 0.00108 | 0.0009646 | 0.0004932 |
| ISE | 0.00278 | 0.002622 | 0.001972 |

Table VIII shows an FLC (without optimization) shows the highest error across all the four metrics, indicating lowest effective sway control among the three strategies. In all the metrics GA-FLC demonstrates moderate improvement over the FLC (without optimization). For instance, GA-FLC reduces IAE to 0.05371 compared to 0.05697 for FLC and much lower than PSO-FLC with 0.03410 which is

36% and 40% GA-FLC and standalone fuzzy respectively.

Percentage improvement was evaluated as in (Aner et al., 2024). The (IAE) criterion integrates the absolute value of error over time. This metric treats all errors equally, regardless of when they occur. Minimizing (IAE) generally leads to a system with a relatively fast response and less oscillation than (ISE), but it does not specifically target long term errors as effectively as (ITAE). (Solihin et al., 2008b).

$$\begin{aligned} & \% \text{ Improvement in IAE} \\ &= \frac{(GA - FLC) - (PSO - FLC)}{(GA - FLC)} \times 100\% \\ &= \frac{0.05371 - 0.03410}{0.05371} \times 100\% = \mathbf{36\%} \end{aligned}$$

$$\begin{aligned} & \% \text{ Improvement in IAE} \\ &= \frac{(FLC \text{ standalone}) - (PSO - FLC)}{(FLC \text{ standalone})} \times 100\% \\ &= \frac{0.056971 - 0.03410}{0.05697} \times 100\% \\ &= \mathbf{40\%} \end{aligned}$$

$$\begin{aligned} & \% \text{ Improvement in ITAE} \\ &= \frac{(GA - FLC) - (PSO - FLC)}{(GA - FLC)} \times 100\% \\ &= \frac{0.03471 - 0.0196}{0.03471} \times 100\% = \mathbf{44\%} \end{aligned}$$

$$\begin{aligned} & \% \text{ Improvement in ITAE} \\ &= \frac{(FLC \text{ standalone}) - (PSO - FLC)}{(FLC \text{ standalone})} \times 100\% \\ &= \frac{0.03881 - 0.0196}{0.03881} \times 100\% = \mathbf{49\%} \end{aligned}$$

The percentage improvement indicated the higher improvement against the standalone FLC (40% and 36%) suggests that GA-FLC performs better than standalone FLC in IAE performance metric. The larger improvements in ITAE (44% and 49%) compared to IAE (36% AND 40%) are particularly significant. ITAE penalizes steady-state error more heavily over time, this indicated that PSO-FLC performs superior long-term error reduction and faster settling time.

This improvement signified that Particle swarm optimization tuned fuzzy logic controller (PSO-FLC) accomplishes the smallest error values, indicating superior sway suppression and control accuracy for the double-girder crane system.

5 Conclusion

The paper was successfully implemented and compared the two Mamdani-types fuzzy logic controllers optimized with Particle swarm optimization (PSO) and Genetic algorithm (GA) for a double-girder overhead crane system. The system's nonlinear dynamics were modelled using the Euler-Lagrange approach, designed for trolley position and payload angle (sway) control. The simulation results demonstrated graphically and numerically that the PSO-FLC outperformed both FLC standalone and GA-FLC in all the performance metrics. For position control PSO-FLC succeeded in fastest settling time 3.8 sec. lowest overshoot 0.039% and smallest error metrics. Likewise for sway angle control PSO-FLC achieved greater performance with the shortest settling time 3.3 sec. smallest overshoot 0.0049% and lowest error values across all four metrics. Numerical analysis demonstrates that PSO-FLC reduced the integral absolute error (IAE) by 36% compared to GA-FLC and by 40% compared to FLC (without optimization). The larger improvements in ITAE (44% and 49%) compared to IAE (36% and 40%) are particularly significant. ITAE penalizes steady-state error more heavily over time, this indicated that PSO-FLC performs superior long-term error reduction and faster settling time.

PSO-FLC proved to be the most efficient control strategy for double-girder crane system, achieving superior accuracy, faster stabilization, improved sway suppression. These findings provide a great impact for industrial settings in implementing an optimised control systems for easy material handling applications where high precision and stability are critical.

REFERENCES

- Abdulhamid, I. B., Muhammad, M., & Khaleel, A. I. (2019). Control of a Double Pendulum Crane System Using PSO-Tuned LQR. *2019 2nd International Conference of the IEEE Nigeria Computer Chapter, NigeriaComputConf 2019*, 1–8. <https://doi.org/10.1109/NigeriaComputConf45974.2019.8949631>
- Adeli, M. (2011). *Anti-swing Control for a Double-Pendulum-Type Overhead Crane Via Parallel Distributed Fuzzy LQR Controller Combined with Genetic Fuzzy Rule Set Selection*. 306–311.
- Ahmad, M. A., Raja Ismail, R. M. T., & Ramli, M. S. (2009). Hybrid input shaping and non-collocated PID control of a gantry crane system: Comparative assessment. *IEEE/ASME International Conference on Advanced Intelligent Mechatronics, AIM*, 1792–1797. <https://doi.org/10.1109/AIM.2009.5229782>
- Alizada, M., & Ozturk, S. (2023). PID and Fuzzy Logic Control of Ball and Beam System Using Particle Swarm Optimization. *World Journal of Engineering and Technology*, 11(04), 859–873. <https://doi.org/10.4236/wjet.2023.114057>
- Aner, E. A., Awad, M. I., & Shehata, O. M. (2024). Performance evaluation of PSO - PID and PSO - FLC for continuum robot 's developed modeling and control. *Scientific Reports*, 0123456789, 1–19. <https://doi.org/10.1038/s41598-023-50551-0>
- Asad, S., Salahat, M., Zalata, M. A., Alia, M., & Rawashdeh, A. Al. (2011). Design of Fuzzy PD-Controlled Overhead Crane System with Anti-Swing Compensation. *Engineering*, 03(07), 755–762. <https://doi.org/10.4236/eng.2011.37091>
- Automatisés, S., Anh, L. Van, Thi, V., & Linh, T. (2024). *Position Control and Anti-Sway of Overhead Crane System with Uncertain Nonlinear Model*. 57(2), 425–431.
- Azmi, N. I. M., Yahya, N. M., Fu, H. J., & Yusoff, W. A. W. (2019). Optimization of the PID-PD parameters of the overhead crane control system by using PSO algorithm. *MATEC Web of Conferences*, 255, 04001. <https://doi.org/10.1051/mateconf/201925504001>
- Cao, W., Zhang, P., Mi, Q., Sun, Y., Shi, J., & Liang, W. (2023). *Optimization of X-axis servo drive performance using PSO fuzzy control technique for double-axis dicing saw*. 1–14.
- Eslleman, E. A., Önal, G., & Kalyoncu, M. (2021). Optimal PID and fuzzy logic based position controller design of an overhead crane using the Bees Algorithm. *SN Applied Sciences*, 3(10). <https://doi.org/10.1007/s42452-021-04793-0>
- Fu, J., Liu, J., Xie, D., & Sun, Z. (2023). Application of Fuzzy PID Based on Stray Lion Swarm Optimization Algorithm in Overhead Crane System Control. *Mathematics*, 11(9). <https://doi.org/10.3390/math11092170>
- Girder, S., & Cranes, B. (2019). *Single Girder vs . Double Girder*.
- Harb, S. F., & Alenany, A. (2025). *Fuzzy Control of a Large Crane Structure Fuzzy Control of a Large Crane Structure*. January. <https://doi.org/10.52549/ijeei.v5i1.256>
- Kozhubaev, Y., Ovchinnikova, E., Krotova, S., Murashov, Y., & Nushtaev, N. (2023). Implementation of a neural network in overhead crane control. *E3S Web of Conferences*, 389. <https://doi.org/10.1051/e3sconf/202338901035>
- Mohamed, K. T., Abdel-razak, M. H., Haraz, E. H., & Ata, A. A. (2022). Fine tuning of a PID controller with inlet derivative filter using Pareto solution for gantry crane systems. *Alexandria Engineering Journal*, 61(9), 6659–6673. <https://doi.org/10.1016/j.aej.2021.12.017>
- Mohammed, A., Altuwais, H., & Alghanim, K. (2023). *An optimized shaped command of overhead crane nonlinear system for rest-to-rest maneuver*. 11(January), 548–554.

- Mohammed, M. A., Maguire, M., & Kim, K. (2021). *Simulated Annealing Algorithm Based Tuning of LQR Controller for Overhead Crane*. 37–42.
- Shao, X., Zhang, J., & Zhang, X. (2019). Takagi-sugeno fuzzy modeling and PSO-Based Robust LQR anti-swing control for overhead crane. *Mathematical Problems in Engineering*, 2019. <https://doi.org/10.1155/2019/4596782>
- Sharma, A. (2020). An intelligent position control using priority based fitness scheme and optimal tuning of fuzzy logic controller parameters with binary bat algorithm for nonlinear gantry crane system. *Journal of Green Engineering*, 10(11), 11687–11700.
- Solihin, M. I., Chuan, C. Y., & Astuti, W. (2019). Optimization of fuzzy logic controller parameters using modern meta-heuristic algorithm for gantry crane system (GCS). *Materials Today: Proceedings*, 29(November 2018), 168–172. <https://doi.org/10.1016/j.matpr.2020.05.641>
- Sun, X., & Xie, Z. (2020). Reinforcement Learning-Based Backstepping Control for Container Cranes. *Mathematical Problems in Engineering*, 2020. <https://doi.org/10.1155/2020/2548319>
- Zhang, T. (2023). Robust Control Method Design for Underactuated Double-Pendulum Overhead Cranes. *Innovation in Science and Technology*, 2(3), 7–25. <https://doi.org/10.56397/ist.2023.05.020>